Nanonewton optical force trap employing anti-reflection coated, high-refractive-index titania microspheres

Anita Jannasch[1], Ahmet F. Demirörs[2†], Peter D. J. van Oostrum[2†], Alfons van Blaaderen[2] and Erik Schäffer[1]*

Optical tweezers are exquisite position and force transducers and are widely used for high-resolution measurements in fields as varied as physics, biology and materials science[1–3]. Typically, small dielectric particles are trapped in a tightly focused laser and are often used as handles for sensitive force measurements. Improvement to the technique has largely focused on improving the instrument and shaping the light beam[1,4], and there has been little work exploring the benefit of customizing the trapped object[5]. Here, we describe how anti-reflection coated, high-refractive-index core–shell particles composed of titania enable single-beam optical trapping with an optical force greater than a nanonewton. The increased force range broadens the scope of feasible optical trapping experiments and will pave the way towards more efficient light-powered miniature machines, tools and applications.

The force range available to optical tweezers limits their applicability, with trapping forces usually spanning from subpiconewtons to ~100 pN (refs 2, 6–8). This range is compatible with the forces that individual molecular machines generate[2], but the mechanical characterization of macromolecules, their assemblies or more complex cellular processes can require much larger forces. For example, protein unfolding, amyloid fibril disruption, cell adhesion and contraction forces may be at the level of a nanonewton or more, which is beyond the capabilities of a standard optical trap[2,8].

The maximum trapping force is limited by the available laser power and trap efficiency. However, an increase in laser power will lead to the generation of heat[9] and, in the case of biological applications, photodamage. Trapping efficiency can be improved by using a Laguerre–Gaussian laser mode[10], for example, or by exploiting near-field effects[11], compensating spherical aberrations[12], choosing the optimal laser expansion[13] or selecting a probe size close to the first Mie resonance[13,14]. Although these measures aim mainly at improving the instrument, all are limited by the material properties and structure of the photonic probe.

The photonic properties of probes can be optimized to increase the trap efficiency. An increase in the refractive index mismatch between the trapped particle and its surrounding medium increases the stabilizing gradient forces and therefore the trapping efficiency. However, there is an upper limit to this mismatch because the destabilizing scattering force increases more strongly with the mismatch than the gradient force does[14,15]. Thus, high-refractive-index particles ($n > 1.73$, immersed in water[15]) cannot be trapped by a single gradient trap[16] unless, as predicted by theory[15], they are photonically

structured to reduce the scattering force—in the simplest case, coated with an anti-reflection layer[14,15]. In previous work[14], silica-coated polystyrene microspheres were found to moderately improve trapping and reduce back-scattered light. For these low-refractive-index materials, however, a coating was not an essential requirement for being able to trap.

In the present work, we took the decisive and difficult step of coating high-refractive-index particles to make previously untrappable probes trappable. We fabricated coated titania particles according to the specifications of Mie theory calculations and characterized them in an optical trap in terms of their trap stiffness per laser power and escape force. We measured a significantly higher trap efficiency, in agreement with the calculations, compared to all other probes in use. According to our measurements, we have extended the applicability of optical tweezers in two ways. First, photodamage in biophysical experiments can be reduced because the same force can be achieved with a much lower laser power. Second, we have brought the force range of optical tweezers into the nanonewton range, which we demonstrate using an optimized optical tweezers set-up at maximum laser power. The trapping properties of our photonically structured, anti-reflection coated titania particles are superior to homogeneous particles, opening up new possibilities for light-driven probes and optical tweezers experiments. Such particles enhance the performance of existing set-ups, increase the overlap in force with other techniques such as atomic force microscopy (AFM), and provide a large dynamic range from subpico- to nanonewton forces.

To design an optimal anti-reflection coated titania microsphere, we used T-matrix and Mie theory calculations (Fig. 1; see Methods). The core and shell size and shell refractive index were optimized to achieve the highest trapping efficiency for a laser wavelength of $\lambda = 1{,}064$ nm. In the calculations, the refractive index of the core was fixed at $n_{core} = 2.3$, which corresponds to the measured value of titania[17], and the shell refractive index was varied. Surprisingly (even for Mie scatterers), the optimal shell refractive index of 1.78 was very close to the geometric mean of 1.75 of the indices from the core and the medium. This geometric mean is expected for an optimal, single-layer anti-reflection coating on flat, macroscopic substrates[18]. For $n_{shell} = 1.78$ (measured value, ~1.7–1.8; ref. 17), we calculated the trap stiffness as a function of core and core–shell diameter (Fig. 1). Without spherical aberrations (see Methods), the highest lateral trap stiffness occurred for a core size of 0.5 ± 0.05 μm and a coating thickness of 0.23 ± 0.04 μm (intense magenta region in Fig. 1a). This anti-reflection coating is

[1]Nanomechanics Group, Biotechnology Center, TU Dresden, Tatzberg 47/49, 01307 Dresden, Germany, [2]Soft Condensed Matter, Debye Institute for Nanomaterials Science, Utrecht University, Princetonplein 5, 3584 CC Utrecht, The Netherlands, [†]Present address: Non-Equilibrium Energy Research Center, Northwestern University, 2145 Sheridan Road, Evanston, Illinois 60208, USA (A.F.D.), Department of NanoBiotechnology, University of Natural Resources and Life Sciences, Muthgasse 11-II, 1190 Vienna, Austria (P.D.J.v.O). *e-mail: erik.schaeffer@biotec.tu-dresden.de
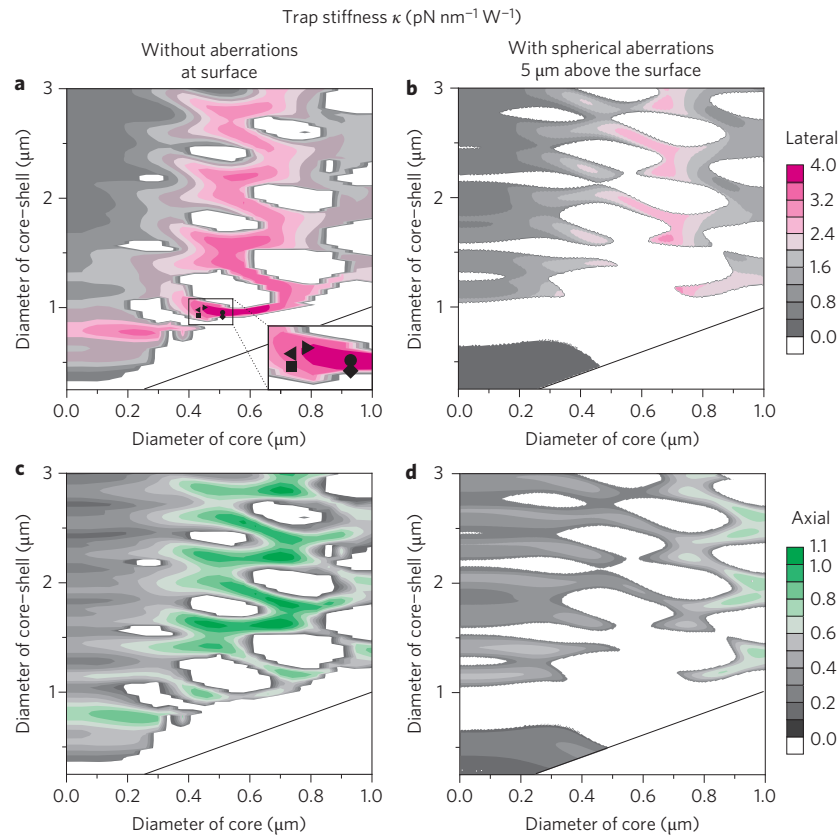
Trap stiffness κ (pN nm^{-1} W^{-1})

Figure 1 | Calculations. Mie theory predictions of lateral (top row) and axial (bottom row) trap stiffness per power in the focus as a function of core diameter and total core–shell diameter (see Methods). White areas correspond to particles that cannot be trapped. The black line demarcates zero shell thickness. **a,c**, *T*-matrix calculations based on the optical tweezers toolbox. The symbols (Table 1, Methods) indicate the size of the fabricated titania core–shell particles. **b,d**, Calculations including spherical aberrations. The geometric focus of the trap is 5 μm away from the glass surface.

significantly thicker than the optimum in a planar configuration: $\lambda/(4n_{shell}) = 0.15$ μm. Thus, calculations were necessary to determine the optimal parameters. Particles with a thinner or thicker shell than the optimal one cannot be trapped according to calculations (white regions in Fig. 1). Also, certain particles—in particular smaller ones—cannot be trapped further away from the surface due to spherical aberrations at the glass–water interface (Fig. 1b,d). Plots for the axial trap stiffness resemble those for the lateral trap stiffness, but with smaller values of the trap stiffness and slightly shifted sizes for the maxima (Fig. 1c,d). Based on these calculations, we fabricated microspheres designed for 'ideal' trapping conditions (no spherical aberrations) using (i) an oil-immersion objective for trapping close to a surface or (ii) a water-immersion objective for trapping far away from a surface. The calculations show that such optimized probes should have an overall diameter of ~1 μm. However, the specifications are stringent with respect to the refractive indices and in particular the shell thickness.

Different batches of titania core–shell particles were synthesized with a core size of ~0.5 μm and a final diameter of ~1 μm (Fig. 2a, inset image). Using a 1.3 NA oil-immersion objective, we could stably trap microspheres in only half the batches at over-filling ratios of ≥1.5 (ref. 13) at distances ≤5 μm away from the surface. This shows how critical the correct parameters are, in particular with respect to spherical aberrations, which are minimal close to the surface. For the microspheres we could trap (marked with black symbols in Fig. 1a, with sizes given in Table 1 in the Methods), we measured the trap stiffness as a function of the total diameter (open symbols in Fig. 2a) and compared the values to those of polystyrene microspheres (hexagons in Fig. 2a). For the titania microspheres we measured a lateral trap stiffness of up to 3.8 pN nm^{-1} W^{-1} and

an axial trap stiffness of up to 0.9 pN nm^{-1} W^{-1} (data not shown). Compared to the maximum lateral (axial) trap stiffness for polystyrene microspheres, this was a twofold (1.3-fold) improvement. The measurements agree well with the predictions (black solid symbols, Fig. 2a) showing that we achieved the maximum possible trapping efficiency. The trap stiffness increased linearly with the laser power in the focus (Fig. 2b). At maximum laser power, a power spectral analysis of the particle motion revealed extremely high corner frequencies. For example, in Fig. 2c the corner frequency is $f_c = 115$ kHz, implying a large trap stiffness $\kappa = 2\pi\gamma f_c = 5.1$ pN nm^{-1}. With such a large trap stiffness, we are able to exert large optical forces.

To demonstrate forces exceeding 1 nN, we performed drag force measurements (Fig. 3). The drag coefficient γ was first measured using our calibration technique, automatically accounting for Faxén's law (see Methods and refs 20,21). The sample was then accelerated relative to the stationary laser until the microsphere escaped the trap while recording both the microsphere detector signal and the stage position (Fig. 3a). From the speed at escape, v_{escape}, we determined the maximum force by $F_{max} = \gamma v_{escape}$. Because of the limiting maximum speed of our piezo-electric translation stage, we had to increase the viscosity of the medium to achieve a sufficiently high drag force to beat the optical trap. For this, we chose water immersion oil with a refractive index comparable to water, but with a 1,000-fold higher viscosity compared to water (see Methods). In the oil, we measured a drag coefficient of $\gamma = 3.9 \pm 0.2$ μN s m^{-1}. At a speed of $v_{escape} \approx 0.3$ mm s^{-1}, the titania core–shell particles escaped from the trap (Fig. 3a). Based on this speed, we measured a maximum force of $F_{max} = 1.20 \pm 0.07$ nN (mean ± s.e.m.) for six different microspheres. The maximum force corresponds to a trapping efficiency of $cF_{max}/(n_{medium}P) = 0.25$,

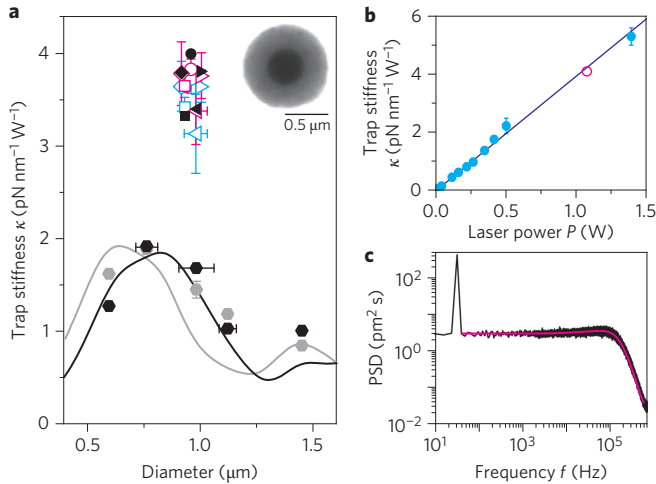**Figure 2 | Measurement of trap stiffness. a**, Trap stiffness per power in the focus of anti-reflection coated titania (blue open symbols, x; magenta open symbols, y; black solid symbols, y theory; different symbols correspond to the batches listed in Table 1) and polystyrene microspheres (grey hexagons, x; black hexagons, y) as a function of microsphere diameter. The plots show mean ± standard deviation. The solid lines (grey, x; black, y) correspond to the T-matrix calculations. Inset: TEM image of a titania core–shell microsphere with a diameter of 0.95 μm. **b**, Trap stiffness κ as a function of laser power P in the focus (blue, water; magenta, oil). The maximum power in water (1.4 W) is higher than in oil (1.1 W) as a result of a different overfilling ratio (see Methods and ref. 13). **c**, Power spectral density (PSD, average of 100 individual power spectra) for a titania microsphere trapped at maximum laser power in water. The spectrum (black line) features a calibration peak at 32 Hz (red line, fit to theory from ref. 19, see Methods).

Table 1 | Dimensions of different titania core–shell microsphere batches as mean ± standard error of the mean (number of measurements) in micrometres. The core diameter was measured by TEM and the core–shell diameter with our optical tweezers calibration. Shell thickness is based on the difference between total and core diameters.

	Core diameter, Anatase titania	Shell thickness, Amorphous titania	Shell thickness, Silica	Total diameter
▷	0.45 ± 0.006 (12)	0.28	–	1.00 ± 0.02 (6)
◁	0.43 ± 0.006 (42)	0.28	–	0.98 ± 0.020 (6)
□	0.43 ± 0.006 (42)	0.25	–	0.93 ± 0.01 (6)
◇	0.51 ± 0.005 (32)	0.20	–	0.91 ± 0.02 (6)
○	0.51 ± 0.007 (21)	0.20	0.02	0.95 ± 0.01 (6)

where c is the speed of light, $P = 1.1\,W$ is the maximum power in oil (Fig. 2b and Methods) and $n_{medium} = 1.33$. Thus, 25% of the light power was used to exert a force. In comparison, efficiencies for silica-coated polystyrene or 3-μm-diameter polystyrene microspheres are only 0.09 and 0.14, respectively[14]. The recorded maximum detector voltage signal at escape is consistent with the maximum value recorded when scanning through an immobilized microsphere (Fig. 3a, inset). Furthermore, as expected[22], the drag force scales almost linearly with the detector signal all the way up to the escape point (Fig. 3b).

Our measurements demonstrate both a significant increase in trap efficiency and escape forces exceeding a nanonewton. The increase in trap stiffness is comparable to the difference between polystyrene and silica[14]. Thus, with our anti-reflection coated titania particles, we have at least a fourfold improvement compared to silica (twofold

compared to polystyrene) particles depending on size[14]. In oil, the nanonewton escape forces were achieved in the regime of the nonlinear displacement response of the trap (Fig. 3c; ref. 22). In water, we achieved a higher maximum laser power in the focus (Fig. 2b and Methods). Therefore, for some microspheres used during calibration in water, we expect to reach a nanonewton even within the linear displacement response of $x^{linear}_{max} \approx 200$ nm (10% deviation, Fig. 3a inset, Fig. 3c). With a trap stiffness of $\kappa = 5.4$ pN nm^{-1}, we estimate the maximum force in the linear response range to be $F^{linear}_{max} = \kappa x^{linear}_{max} \approx 1$ nN (Fig. 3c). The ~1 μm diameter of our particles is a compromise between small particles that have a fast response and large particles that provide a contact point for lateral, biomolecule attachment beyond the trapping focus. Microspheres with a larger core diameter of ~0.75 μm and outer diameter of ~1.2 μm would also enable trapping in the presence of spherical aberrations, but with a ~20% lower efficiency compared to the maximum (Fig. 1). Fabricating larger particles with high trapping efficiencies should be possible (Fig. 1), although the synthesis of a homogeneous thick shell is non-trivial and has not been possible in a general way with a relatively high, non-absorbing refractive index (>1.7) until recently[17]. For smaller diameters with preserved, high trap efficiency, the trapping wavelength would have to be reduced, which may increase phototoxicity.
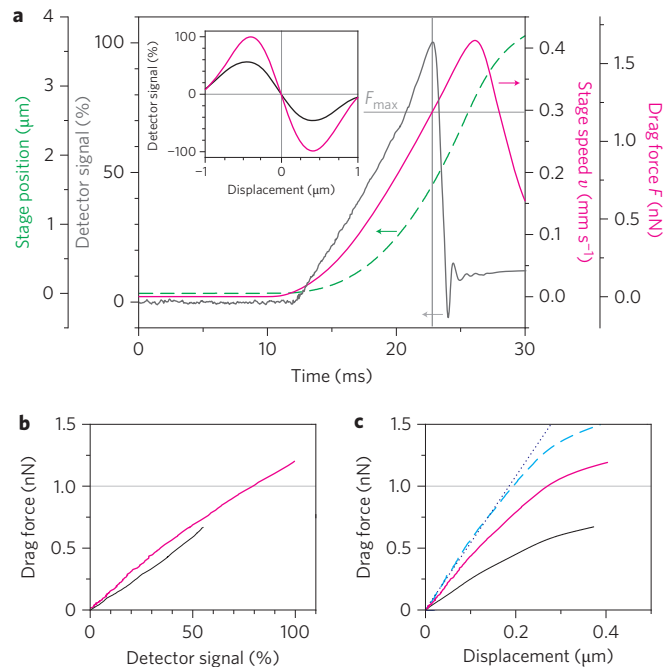

Figure 3 | Escape force measurements in oil. a, Simultaneous recording of the microsphere detector signal (grey line) and sample stage position (green dashed line) as a function of time. Stage speed v_{stage} corresponds to the derivative of the stage position. The drag force is determined from $F = \gamma v_{stage}$ using the measured drag coefficient γ. The vertical grey line indicates the escape time and the horizontal grey line the escape speed and maximum force. Ordinate zeros are offset for clarity. Inset: lateral detector response for an immobilized 1-μm-diameter titania particle (red line) and a 0.992-μm-diameter polystyrene particle (black line) as a function of displacement relative to the trap centre. **b,c**, Drag force as a function of detector signal (**b**) and displacement (**c**) inferred from a scan through an immobilized microsphere (inset in **a**). At the highest detector signal, the microsphere escaped the trap. When the escape force of the titania microsphere was scaled to the maximum trap stiffness measured in water (blue dashed line), the force was linear in displacement (dotted line) up to ~1 nN. All detector voltage signals were scaled by the maximum voltage $V^{titania}_{max}$ recorded for the titania microspheres.

The high trap efficiency is useful in reducing radiation damage in the case of sensitive samples, in increasing the number of simultaneously trappable particles when splitting the laser into multiple traps[1], or in generating very high optical forces. For high force measurements, laser-induced heating[9] might be a concern. For the measurements in oil, we estimate that we heated the sample by ∼8 °C (see Methods). In water at maximum laser power, we heated the sample by 3 °C close to the surface and 16 °C far away from the surface—the glass surface acting as a heat sink[9,19]. To reduce heating, experiments could be performed at a different (smaller) trapping wavelength, in heavy water[23] or in other liquids. Titanium with a native oxide layer is often used as a biocompatible material and can be functionalized with biomolecules[24], so our anti-reflection coated titania microspheres should be useful for biological applications. Furthermore, an additional thin silica coating on the titania core–shell particles (batch ○, Table 1) did not negatively influence the trapping, and silica particles can be readily used for biological experiments (for example, refs 2,14).

The high trap stiffness, in combination with significantly larger microspheres than ours, should facilitate new experiments, for example to measure resonances associated with the coloured nature of the thermal noise that drives Brownian motion[19,25]. Moreover, it has already been demonstrated that high-index particles can also be detected in three dimensions with unprecedented accuracy using holography, which is fully compatible with a tweezers set-up[26]. To increase the working distance, counter-propagating traps with low-NA lenses have been used. Trapping our coated microspheres in such a geometry should be possible. However, we expect only minor improvements compared to uncoated, high-refractive-index particles[16]. The advantage of a coating is that lower-NA objectives should already be sufficient for trapping in single-beam tweezers[15], making the technique simpler and more compatible with other methods. Experiments so far restricted to AFM are also feasible with high-resolution optical traps. Apart from three-dimensional scanning with a 'stiff' photonic probe, optical tweezers experiments are feasible in the nanonewton force range with subpiconewton resolution, for instance for protein unfolding or intra- and intercellular measurements, can complement or replace AFM approaches, and can open up new possibilities that take advantage of the three-dimensional capabilities of optical trapping. Sculpturing optimized photonic structures[5], for example, using two-photon polymerization[27] to generate gears, rotors, pumps, cell pokers[28] and so on, will be an essential ingredient in the creation of complex, light-driven miniature tools and objects.

Methods

Theory. Two methods were used to calculate the trap efficiency in terms of the trap stiffness per power. Both calculations are based on the scattering of light by small particles as described either by the T-matrix method[14,29] or generalized Lorentz–Mie theory[16]. For both calculations, the following parameters are used: refractive indices $n_{core} = 2.3$, $n_{shell} = 1.78$ and $n_{H_2O} = 1.326$, at a laser wavelength of 1,064 nm. A thin silica layer in one batch of particles (Table 1) was neglected in the calculations. The T-matrix calculation was based on an extended version of the optical tweezers toolbox[14,29]. For the toolbox, we used an effective numerical aperture of 1.25, an overfilling described by a truncation angle of $\theta = 80°$, and a polarization in the y-direction (the plotted lateral direction in Fig. 1). Spherical aberrations occurring at the glass–water interface were not considered in this model, and a least-squares fit was used to produce a Helmholtz beam with a far field matching that of the incident beam focused by the objective. The second calculation[16] included the effect of spherical aberrations produced by refraction at the glass–water interface. For this calculation, the geometric focus of the trap was 5 μm away from the glass surface. The numerical aperture of the objective was 1.22 and the ratio between the focal lengths and the beam waist was 0.903. With these parameters, both methods gave consistent results at the surface where spherical aberrations are minimal.

Optical tweezers set-up. Measurements were performed in single-beam optical tweezers optimized for stability and performance[13,30]. Briefly, for trapping, we used a laser with 4.5 W output power at 1,064 nm and a position-sensitive photodiode for back-focal-plane detection. The laser was focused by an oil-immersion objective (CFI S Fluor ×100, 0.7–1.3NA, Nikon) to a diffraction-limited spot[13], and the

scattered light was collected by an identical objective. The temperature of the objectives was stabilized with feedback to 29.000 °C (ref. 30). For trap stiffness (drag force) measurements, the overfilling of the objective[13] was 1.5 (2.0) with a maximum power of 1.4 W (1.1 W) in the focus. The larger filling ratio enabled the microspheres in oil to be trapped more easily.

Synthesis. The synthesis of the core–shell particles is described in detail in ref. 17. Briefly, we coated anatase titania microspheres ($n = 2.3$; ref. 17) with amorphous titania ($n = 1.5$). The particles were then dried at 50 °C for 30 min to increase the refractive index of the amorphous titania to ∼1.7–1.8. The refractive indices were determined with static light-scattering measurements and holographic microscopy[26]. One batch of particles was finally coated with a thin silica shell ($n = 1.45$). Transmission electron microscopy (TEM) revealed homogeneous core sizes and coatings (Fig. 2a, inset, and ref. 17). Particles that could be successfully trapped are listed in Table 1.

Sample preparation and calibration. We prepared samples as described in refs 14 and 21. Flow cells were composed of two cover slips (18 mm² and 22 mm²) separated by two parafilm stripes forming a $3 \times 18 \times 0.1$ mm³ channel. All microspheres were washed in distilled water (aqua bidestillata, 18.2 MΩ cm). All measurements were carried out in distilled water close to the glass surface (microsphere centre–surface distance, ∼2 μm). For each microsphere type, we acquired data for at least six microspheres. Calibration was based on a drag force method using a small sinusoidal stage movement combined with power spectral analysis[20,21]. Using the calibration, we measured the distance to the surface, the drag coefficient γ and associated diameter of the microsphere, the displacement sensitivity of the photodiode, and the trap stiffness κ for all spatial directions[21]. Calibration measurements were performed at ∼5% laser power (output power, 0.23 W). Control measurements confirmed the linearity between trap stiffness and laser power (Fig. 2b). For comparison, we used polystyrene microspheres with diameters of 0.6–1.5 μm ($n_{PS} = 1.57$, Bangs Laboratories). For the escape force measurements, we used 100% laser power (output power, 4.5 W). The particles were dried at room temperature for 60 min and then resuspended in water immersion oil ($n = 1.33$; Immersol W, Zeiss) with a dynamic viscosity of 1.08 Pa at 20 °C (0.32 Pa s at 40 °C). To achieve a nearly linear increase in drag force with time, the piezo translation stage holding the sample was accelerated at 40 mm s⁻² relative to the stationary laser.

Laser-induced heating in oil. The amount of laser-induced heating when trapping in immersion oil was estimated according to the following calculation. With the drag coefficient measured in oil, we calculated an oil viscosity of 0.42 ± 0.03 Pa s using the average microsphere radius (batch ▷, Table 1), also accounting for the distance to the surface[21]. Based on a linear interpolation between manufacturer-given values (see above paragraph), this viscosity corresponded to a temperature of 37 ± 1 °C and the stated increase in temperature.

References

1. Padgett, M. & Bowman, R. Tweezers with a twist. *Nature Photon.* **5,** 343–348 (2011).
2. Fazal, F. M. & Block, S. M. Optical tweezers study life under tension. *Nature Photon.* **5,** 318–321 (2011).
3. Grier, D. G. Optical tweezers in colloid and interface science. *Curr. Opin. Colloid Interface Sci.* **2,** 264–270 (1997).
4. Dholakia, K. & Čižmár, T. Shaping the future of manipulation. *Nature Photon.* **5,** 335–342 (2011).
5. Glückstad, J. Optical manipulation: sculpting the object. *Nature Photon.* **5,** 7–8 (2011).
6. Smith, S. B., Cui, Y. J. & Bustamante, C. Overstretching B-DNA: the elastic response of individual double-stranded and single-stranded DNA molecules. *Science* **271,** 795–799 (1996).
7. Maier, B., Potter, L., So, M., Seifert, H. S. & Sheetz, M. P. Single pilus motor forces exceed 100 pN. *Proc. Natl Acad. Sci. USA* **99,** 16012–16017 (2002).
8. Dong, J., Castro, C. E., Boyce, M. C., Lang, M. J. & Lindquist, S. Optical trapping with high forces reveals unexpected behaviors of prion fibrils. *Nature Struct. Mol. Biol.* **17,** 1422–1430 (2010).
9. Peterman, E., Gittes, F. & Schmidt, C. F. Laser-induced heating in optical traps. *Biophys. J.* **84,** 1308–1316 (2003).
10. Simpson, N. B., McGloin, D., Dholakia, K., Allen, L. & Padgett, M. J. Optical tweezers with increased axial trapping efficiency. *J. Mod. Opt.* **45,** 1943–1949 (1998).
11. Juan, M. L., Righini, M. & Quidant, R. Plasmon nano-optical tweezers. *Nature Photon.* **5,** 349–356 (2011).
12. Reihani, S. N. & Oddershede, L. B. Optimizing immersion media refractive index improves optical trapping by compensating spherical aberrations. *Opt. Lett.* **32,** 1998–2000 (2007).

13. Mahamdeh, M., Campos, C. P. & Schäffer, E. Under-filling trapping objectives optimizes the use of the available laser power in optical tweezers. *Opt. Express* **19**, 11759–11768 (2011).
14. Bormuth, V. *et al.* Optical trapping of coated microspheres. *Opt. Express* **16**, 13831–13844 (2008).
15. Hu, Y., Nieminen, T. A., Heckenberg, N. R. & Rubinsztein-Dunlop, H. Antireflection coating for improved optical trapping. *J. Appl. Phys.* **103**, 093119 (2008).
16. van der Horst, A., van Oostrum, P. D. J., Moroz, A., van Blaaderen, A. & Dogterom, M. High trapping forces for high-refractive index particles trapped in dynamic arrays of counterpropagating optical tweezers. *Appl. Opt.* **47**, 3196–3202 (2008).
17. Demirörs, A. F. *et al.* Seeded growth of titania colloids with refractive index tunability and fluorophore-free luminescence. *Langmuir* **27**, 1626–1634 (2011).
18. Walheim, S., Schäffer, E., Mlynek, J. & Steiner, U. Nanophase-separated polymer films as high-performance antireflection coatings. *Science* **283**, 520–522 (1999).
19. Jannasch, A., Mahamdeh, M. & Schäffer, E. Inertial effects of a small Brownian particle cause a colored power spectral density of thermal noise. *Phys. Rev. Lett.* **107**, 228301 (2011).
20. Tolić-Nørrelykke, S. F. *et al.* Calibration of optical tweezers with positional detection in the back focal plane. *Rev. Sci. Instrum.* **77**, 103101 (2006).
21. Schäffer, E., Nørrelykke, S. & Howard, J. Surface forces and drag coefficients of microspheres near a plane surface measured with optical tweezers. *Langmuir* **23**, 3654–3665 (2007).
22. Jahnel, M., Behrndt, M., Jannasch, A., Schäffer, E. & Grill, S. W. Measuring the complete force field of an optical trap. *Opt. Lett.* **36**, 1260–1262 (2011).
23. Moffitt, J. *et al.* Intersubunit coordination in a homomeric ring ATPase. *Nature* **457**, 446–450 (2009).
24. Geiseler, B. & Fruk, L. Bifunctional catechol based linkers for modification of TiO$_2$ surfaces. *J. Mater. Chem.* **22**, 735–741 (2012).
25. Franosch, T. *et al.* Resonances arising from hydrodynamic memory in Brownian motion. *Nature* **478**, 85–88 (2011).
26. Lee, S.-H. *et al.* Characterizing and tracking single colloidal particles with video holographic microscopy. *Opt. Express* **15**, 18275–18282 (2007).
27. Galajda, P. & Ormos, P. Complex micromachines produced and driven by light. *Appl. Phys. Lett.* **78**, 249–251 (2001).
28. Palima, D. *et al.* Wave-guided optical waveguides. *Opt. Express* **20**, 2004–2014 (2012).
29. Nieminen, T. A. *et al.* Optical tweezers computational toolbox. *J. Opt. A* **9**, S196–S203 (2007).
30. Mahamdeh, M. & Schäffer, E. Optical tweezers with millikelvin precision of temperature-controlled objectives and base-pair resolution. *Opt. Express* **17**, 17190–17199 (2009).

Acknowledgements

Author contributions

E.S. designed research. A.J. performed measurements. A.J. and A.F.D. synthesized the particles. A.v.B. advised on the synthesis. A.J. and P.D.J.v.O. performed theoretical calculations. A.J. and E.S. analysed the data and wrote the manuscript.

Additional information

The authors declare no competing financial interests. Reprints and permission information is available online at http://www.nature.com/reprints. Correspondence and requests for materials should be addressed to E.S.